Synthesis and Field-Emission Properties of Ga_2O_3−C Nanocables

Jinhua Zhan,* Yoshio Bando, Junqing Hu, Yubao Li, and Dmitri Golberg

Advanced Materials Laboratory, National Institute for Materials Science, Namiki 1-1, Tsukuba, Ibaraki 305-0044, Japan

Received July 6, 2004. Revised Manuscript Received September 15, 2004

Uniform Ga_2O_3−C nanocables with an average core diameter of 40 nm, wall thickness of 6 nm, and lengths of up to dozens of μm were generated via co-thermal evaporation of gallium oxide and activated carbon powder. The nanocable formation is discussed based on thermodynamics and crystallography. Gallium oxide and carbon generate gaseous Ga_2O and CO at a higher temperature; they then recombine to form Ga_2O_3 and C. The simultaneous generation of Ga_2O_3 and C ensures continuous uniform coatings of carbon on gallium oxide nanowires. Field-emission measurements indicated that the nanocables exhibited an unusual sharp increase in emission current density near the threshold field.

Introduction

The synthesis of one-dimensional nanostructures has attracted significant attention due to their space confined properties.[1] One-dimensional nanostructures such as rods, wires, belts, and tubes can be fabricated through a number of advanced nanolithographic techniques, thermal evaporation, and solution-based methods.[2] Due to the growing demands of nanoscale electronics, it is crucial to assemble known functional materials in either radial or axial directions within a single nanoscale building block to form heterostructures, namely coaxial nanocables. Such cables often exhibit novel functional properties as compared to the individual materials constituting them. Many works have been focused on semiconductor−core nanoscale heterostructures: SiC/SiO_2−BN−C, Si/SiO_2−C, and SiC−C nanocables have been synthesized via a reactive laser ablation or coating silicon carbide nanowires with carbon.[3−6]

Gallium oxide, β-Ga_2O_3, is a wide-band-gap semiconductor with a band gap of approximately 4.9 eV at room temperature.[7] Interestingly, the magnetism due to conduction electron spins in the material can exhibit an original memory effect within a temperature range 4−293 K. Syntheses of one-dimensional gallium oxide nanostructures have been reported.[8−13] Herein we report on the synthesis of Ga_2O_3−C nanocables via direct thermal evaporation of gallium oxide and activated carbon powder and the analysis of their field-emission performance.

Experimental Section

The Ga_2O_3−C nanocables were synthesized in a vertical induction furnace. The furnace consisted of a fused-quartz tube and an induction-heated cylinder made of high-purity graphite coated with a C fiber thermo-insulating layer. The system has an inlet C pipe and an outlet C pipe on its top and base, respectively. A carbon plate was placed below the outlet pipe. A graphite crucible, containing 0.40 g Ga_2O_3 and 0.05 g activated carbon powder was placed at the center cylinder zone. After evacuation of the quartz tube to ~0.1 Torr, a pure N_2 flow was set within the carbon cylinder at a constant rate of 1000 sccm. The furnace was heated to and kept at 1300 °C for 1 h. After the reaction was terminated and the furnace cooled to the room temperature, a gray product was collected from the carbon plate in the carbon induction-heated cylinder. The yield of products is about 10% based on the amount of precursor Ga_2O_3 powder.

The product was characterized using X-ray powder diffraction (XRD; RINT 2200) with Cu Kα radiation. The morphology of the product was observed using a JSM-6700F scanning electron microscope (SEM) operated at 10−20 kV. The product was ultrasonically dispersed in ethanol and transferred to a carbon-coated copper grid for transmission electron microscopy (TEM) observations. A field-emission JEM-3000F high-resolution electron microscope operated at 300 kV equipped with an energy-dispersive X-ray spectrometer (EDS) was employed to perform the microanalysis. Field-emission measurements of

* Corresponding author. Fax: 81-29-851-6280. E-mail: zhan.jinhua@nims.go.jp.

(1) (a) Xia, Y.; Yang, P.; Sun, Y.; Wu, Y.; Mayers, B.; Gates, B.; Yin, Y.; Kim, F.; Yan, Y. *Adv. Mater.* **2003**, *15*, 353. (b) Dai, H. *Acc. Chem. Res*. **2002**, *35*, 1035. (c) Sloan, J.; Kirkland, A. I.; Hutchison, J. L.; Green, M. L. H. *Chem. Commun*. **2002**, 1319. (d) Han, W. Q.; Fan, S. S.; Li, Q. Q.; Hu, Y. D. *Science* **1997**, *277*, 1287. (e) Dai, H. J.; Wong, E. W.; Lu, Y. Z.; Fan, S. S.; Lieber, C. M. *Nature* **1995**, *375*, 769. (f) Rao, C. N. R.; Deepak, F. L.; Gundiah, G.; Govindaraj, A. *Prog. Solid State Chem.* **2003**, *31*, 5.

(2) (a) Patzke, G. R.; Krumeich, F.; Nesper, R. *Angew. Chem., Int. Ed.* **2002**, *41*, 2446. (b) Hu, J.; Odom, T. W.; Lieber, C. M. *Acc. Chem. Res.* **1999**, *32*, 435. (c) Pan, Z. W.; Dai, Z. R.; Wang, Z. L. *Science* **2001**, *291*, 1947. (d) Zhan, J.; Yang, X.; Wang, D.; Li, S.; Xia, Y.; Qian, Y. *Adv. Mater.* **2000**, *12*, 1348. (e) Zhang, R. Q.; Lifshitz, Y.; Lee, S. T. *Adv. Mater.* **2003**, *15*, 635.

(3) Zhang, Y.; Suenaga, K.; Colliex, C.; Iijima, S. *Science* **1998**, *281*, 973.

(4) Shi, W. S.; Peng, H. Y.; Xu, L.; Wang, N.; Tang, Y. H. H.; Lee, S. T. *Adv. Mater.* **2000**, *12*, 1927.

(5) Kim, H. Y.; Park, J.; Yang, Y. *Chem. Commun.* **2003**, 256.

(6) Li, Y.; Bando, Y.; Golberg, D. *Adv. Mater.* **2004**, *16*, 93.

(7) Binet, L.; Gourier, D. *J. Phys. Chem. Solids* **1998**, *59*, 1241.

(8) Dai, Z. R.; Pan, Z. W.; Wang, Z. L. *J. Phys. Chem. B* **2002**, *106*, 902.

(9) Sharma, S.; Sunkara, M. K. *J. Am. Chem. Soc.* **2002**, *124*, 12288.

(10) Chun, H. J.; Choi, Y. S.; Bae, S. Y.; Seo, H. W.; Hong, S. J.; Park, J.; Yang, H. *J. Phys. Chem. B* **2003**, *107*, 9042.

(11) Liang, C. H.; Meng, G. W.; Wang, G. Z.; Wang, Y. W.; Zhang, L. D.; Zhang, S. Y. *Appl. Phys. Lett.* **2001**, *78*, 3202.

(12) Zhang, H. Z.; Kong, Y. C.; Wang, Y. Z.; Du, X.; Bai, Z. G.; Wang, J. J.; Yu, D. P.; Ding, Y.; Hang, Q. L.; Feng, S. Q. *Solid State Commun.* **1999**, *109*, 677.

(13) Ma, R.; Bando, Y. *Chem. Phys. Lett.* **2003**, *367*, 219.

10.1021/cm048909u CCC: $27.50
Published on Web 11/03/2004

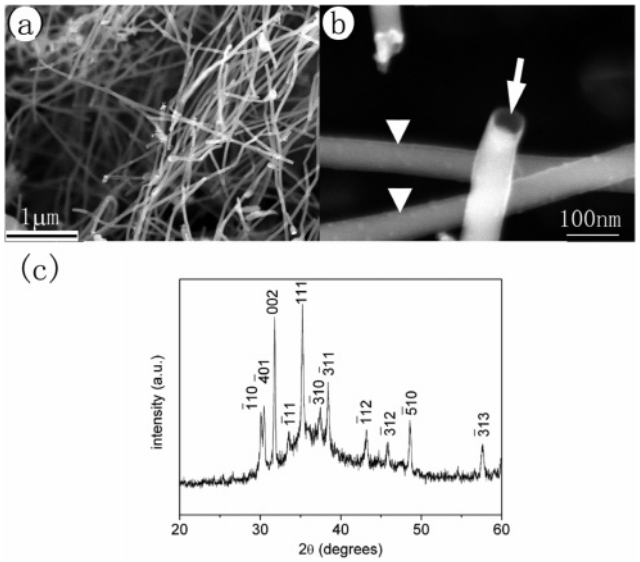

Figure 1. (a) SEM image of as-obtained Ga_2O_3−C nanocables; (b) typical SEM image showing the open end of a Ga_2O_3−C nanocable; and (c) XRD pattern of an as-obtained product.

the nanocables were conducted in a vacuum chamber at a pressure of $\sim 6.0 \times 10^{-5}$ Pa. A rodlike aluminum probe with 1 mm^2 in cross section was used as the anode. The as-obtained nanocables were used as the cathode. A dc voltage sweeping from 0 to 1100 V was applied to the sample.

Results and Discussion

A representative SEM image of a sample is shown in Figure 1a, which indicates that the product is composed of wire-like nanostructures with a length of up to several micrometers. Detailed SEM analysis reveals that the wire-like nanostructures have core−shell structures and thus can be defined as nanocables. Figure 1b shows the open end of a nanocable, indicated by the arrow. A uniform continuous filling of the nanocable is marked with the "diamond"-like symbols in Figure 1b. The diameter of the nanocables is approximately 50 nm. The X-ray diffraction (XRD) pattern of the product shown in Figure 1c reveals the formation of a crystalline gallium oxide.

Detailed structural and chemical analysis of individual composite nanowires was carried out using high-resolution TEM (HRTEM). Figure 2a, a TEM image of a typical as-obtained Ga_2O_3−C nanocable, displays that its core diameter is approximately 40 nm, whereas its sheath is 6 nm thick. The corresponding selected-area electron diffraction pattern in Figure 2b suggests that the cable is a single crystal. All the spots on the pattern can be indexed as those natural for the [101] zone axis of β-Ga_2O_3. EDS analysis also indicates that the cable-like nanostructures are composed of Ga and O. The EDS spectrum of the Ga_2O_3−C nanocable is shown in Figure 2c. A high-resolution TEM image taken from the core

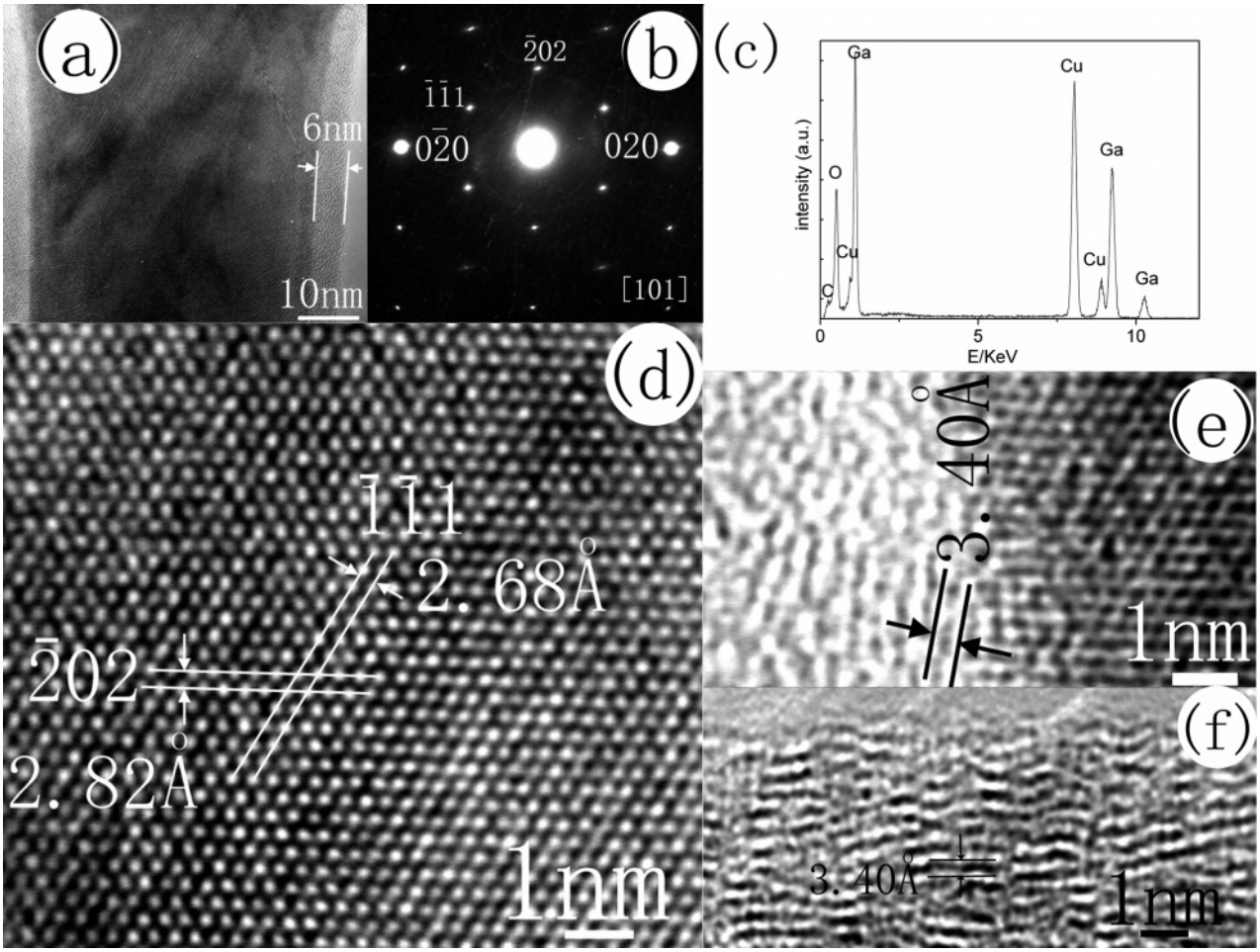

Figure 2. (a) Typical TEM image of an as-obtained Ga_2O_3−C nanocable; (b) selected-area electron diffraction (SAED) pattern of the nanocable; (c) EDS spectrum of the Ga_2O_3−C nanocable; (d) HRTEM image of the nanocable core; (e) HRTEM image of the nanocable wall-core interface; and (f) HRTEM image of the nanocable wall.

is depicted in Figure 2d. The HRTEM image of the core indicates clearly-resolved interplanar distances of 2.82 and 2.68 Å, corresponding to the $(\bar{2}02)$ and $(\bar{1}0\bar{1})$ lattice spacings, respectively. HRTEM analysis also reveals that the crystalline Ga_2O_3 core is free from dislocations or stacking faults. Figure 2e indicates that the crystalline Ga_2O_3 core has a sharp interface with the carbon wall. A high-resolution TEM image taken from the longitudinal edge of a nanocable is shown in Figure 2f, which displays that the thin wall around the core has a layered structure. The interlayer distance of approximately 3.40 Å coincides with that between adjacent basal planes in graphite crystals. In contrast with well-crystallized graphite layers in carbon nanotubes, the carbon walls in these nanocables are less ordered. As revealed by the HRTEM observation and SAED pattern, the growth direction of crystalline Ga_2O_3 core is nearly perpendicular to the $(\bar{2}02)$ crystal planes, namely$(\bar{2}02)^*$.

β-Ga_2O_3 is a thermodynamically stable form of gallium oxide in ambient conditions. It has a monoclinic unit cell and belongs to the space group $C2/m$.[14] The lattice constants of β-Ga_2O_3 are $a = 12.227$ Å, $b = 3.0389$ Å, $c = 5.8079$ Å, $\beta = 103.82°$. The O atoms have a distorted cubic close packing in β-Ga_2O_3 crystals, which contain two crystallographically different Ga atoms in the asymmetric unit, one with tetrahedral coordination geometry (Ga1) and the other with octahedral coordination geometry (Ga2). The octahedrons share edges to form double chains parallel to the *b*-axis, connected by corner-sharing tetrahedrons. Figure 3a displays the structural model of β-Ga_2O_3 crystal viewed along the [1 0 1] axis. The $(\bar{2}02)^*$ plane and *b*-axis are shown in Figure 3a. As documented by the structural model, the double chains of edge-sharing octahedrons and chains of corner-sharing tetrahedrons stack alternately along the $(\bar{2}02)^*$ planes forming corner-sharing connections. The growth direction of crystalline Ga_2O_3 core is dependent on this crystallographic feature. The lattice constant (12.227 Å) of β-Ga_2O_3 is nearly 10 times larger than the interplanar distance (1.234 Å) between the (110) planes in graphite. The $(\bar{2}02)$ interplanar distance of β-Ga_2O_3 is nearly two times larger than the sp^2 C−C bond length (1.421 Å) in graphite. Figure 3b and c show the crystallographic relationship between β-Ga_2O_3 and a single graphene sheet. The white parallelogram on a graphene sheet shown in Figure 3c is very close to that in 3b so that it is reasonable to think carbon can form uniform coating on β-Ga_2O_3 crystals.

It is well-known that the inner cavity of an open carbon nanotube can be used to accommodate foreign elements or compounds.[15−18] It is difficult though to create filling via capillarity over distances more than 100 nm due to the fact that the filling terminates once the inner hydrostatic pressure equilibrates the outer pressure. The continuous filling of carbon nanotubes reported here is suggested to be a result of simultaneous crystallization of gallium oxide and carbon nanotubes

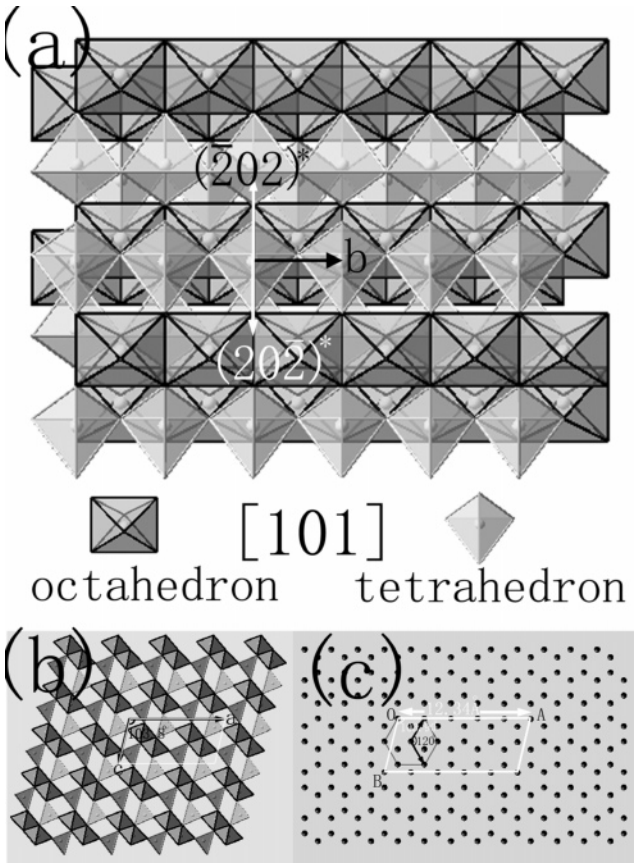

Figure 3. (a) Scheme of β-Ga_2O_3 crystal structure viewed along the [101] direction. (b) Structural model of the (020) crystal plane of β-Ga_2O_3 crystal. (c) Structural model displaying the structural relationship between of β-Ga_2O_3 and a single graphene sheet. The white parallelogram on a graphene sheet corresponds to that in (b).

in line with the following chemical reactions. These reactions are assumed based on the thermodynamical properties consecutively noted in the parentheses below:

$$Ga_2O_3 + 2C\ (graphite) \rightarrow Ga_2O(g) + 2CO\ (g) \quad (1)$$

$$(\Delta G^\circ_{1600K} = -123.222\ kJ/mol,\ \log K_{1600K} = 4.022)$$

$$Ga_2O(g) + 2CO\ (g) \rightarrow Ga_2O_3 + 2C\ (graphite) \quad (2)$$

$$(\Delta G^\circ_{1000K} = -198.173\ kJ/mol,\ \log K_{1000K} = 10.35)$$

As revealed by the reaction 1, the total entropy considerably increases to form gaseous Ga_2O and CO. It is favorable for the reaction 1 to increase its temperature. At a temperature as high as 1600 K, Ga_2O_3 spontaneously reacts with a carbon powder to form gaseous Ga_2O and CO due to negative Gibbs free energy. Being carried by the N_2 gas flow to a lower temperature region, gaseous Ga_2O and CO can recombine to form crystalline gallium oxide and carbon nanotubes in accord with the reaction 2. Ga_2O_3 grows along a direction perpendicular to the $(\bar{2}02)$ plane, meanwhile, carbon is coated on its surface.

Field-emission measurements of the nanocables were conducted in a vacuum chamber at a pressure of ~6.0×10^{-5} Pa. Figure 4 shows emission current density, *J*, versus applied field curves at an anode-sample distance of 97 μm. The Fowler−Nordheim (F−N) plot of the data

(14) Geller, S. *J. Chem. Phys.* **1960**, *33*, 676.
(15) Ajayan, P. M.; Ebbesen, T. W.; Ichihashi, T.; Iijima, S.; Tanigaki, K.; Hiura, H. *Nature* **1993**, *362*, 522.
(16) Tsang, C.; Chen, K.; Harris, P. J. F.; Green, M. L. H. *Nature* **1994**, *372*, 160.
(17) Monthioux, M. *Carbon* **2002**, *40*, 1809.
(18) Pham-Huu, C.; Keller, N.; Estournès, C.; Ehret, G.; Ledoux, M. J. *Chem. Commun.* **2002**, 1882.

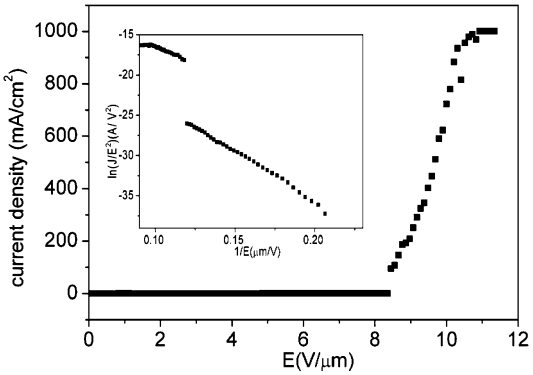

Figure 4. Field-emission I–V curve obtained on the nanocables. The inset depicts the F–N plot, which is composed of two discrete straight lines.

is shown in the inset of Figure 4. A turn-on field 7.73 V/μm and a threshold field of 8.45 V/μm were obtained. This value is compatible to that of carbon nanotubes.[19–21] The behavior of the emission current versus the applied voltage was analyzed using the Fowler–Nordheim equation,[22] $\ln(J/E^2) = -(B\phi^{3/2}/\beta)E^{-1} + \ln(A\alpha\beta^2/\phi)$, where J is the current density, E is the applied field (V/d), ϕ is the work function, B and A are constants, α is the effective emission area, and β is the F–N enhancement factor. The slope of the Fowler–Nordheim (F–N) plot shown in the Figure 4 inset indicates that the emission is generally consistent with the F–N mechanism by exhibiting linear dependence, but the F–N curve is composed of two discrete straight lines separated at the threshold field. The sharp increase in the emission current at the threshold field may be due to the fact that the interaction between the carbon shells and the gallium oxide cores starts to contribute to the total emission current at a higher field. It has been reported that the carbon nanotube films had an emission current density of 100 mA/cm^2 at an electric field of 10 V/μm[19] and the needle-shaped SiC nanowires had a field emission current density of 30.8 mA/cm^2 at an electric field of 9.6 V/μm.[23] The emission current density of the nanocables can be as high as 722.5 mA/cm^2 at an electric field of 10 V/μm, indicating that the as-obtained nanocables are a prospective candidate for field-emitters.

In summary, uniform Ga_2O_3–C coaxial nanocables were synthesized through direct thermal evaporation of gallium oxide and activated carbon powder at 1300 °C. The diameter of the β-Ga_2O_3 cores is approximately 40 nm and their length is up to dozens of micrometers. Thickness of the carbon outer sheath is approximately 6 nm. The growth of Ga_2O_3–C coaxial nanocables is explained by keeping in mind the thermodynamical properties and relevant crystallography. The nanocables exhibited a sharp increase in emission current density near the threshold field and showed an emission current density as high as 722.5 mA/cm^2 at an electric field of 10 V/μm.

Acknowledgment. We thank Dr. Yoichiro Uemura and Keiji Kurashima for technical support.

CM048909U

(19) Xu, X. P.; Brandes, G. R. *Appl. Phys. Lett.* **1999**, *74*, 2549.
(20) Fan, S. S.; Chapline, M. G.; Franklin, N. R.; Tombler, T. W.; Cassell, A. M.; Dai, H. J. *Science* **1997**, *283*, 512.
(21) Collins, P. G.; Zettl, A. *Phys. Rev. B* **1997**, *55*, 9391.
(22) Marcus, R. B.; Ravi, T. S.; Gmitter, T.; Busta, H. H.; Niccum, J. T.; Chin, K. K.; Liu, D. *IEEE Trans. Electron Devices* **1991**, *38*, 2289.
(23) Wu, Z. S.; Deng, S. Z.; Xu, N. S.; Chen, J.; Zhou, J.; Chen, J. *Appl. Phys. Lett.* **2002**, *80*, 3829.